VOLUMETRIC IMAGE PROCESSING BY THREE-DIMENSIONAL FILTERS

Dimitar G. Valchev

Technical University of Varna
1 Studentska St, 9010 Varna, Bulgaria
Phone: +359 52 383 596; E-mail: dvalchev@ece.neu.edu

Abstract

This paper develops filter derivation for volumetric image processing both for the cases of separable and non-separable three-dimensional filters. Such filters find major applications in the fields of computed tomography and magnetic resonance imaging systems, as well as in other subsurface sensing techniques.

1. INTRODUCTION

Volumetric images arise in many applications such as computer tomography imaging and subsurface sensing of various hidden spaces. Volumetric images are represented as three-dimensional (3-D) arrays of voxel values. They provide realistic representations of real world solids as true 3-D images, not just 2-D projections onto a planar display. Being 3-D signals, volumetric images are subject to 3-D signal processing. The various filtering techniques from 2-D signal processing may be extended to three dimensions.

Basic to the filter characterization methodology is the derivation of the impulse response of an ideal lowpass 3-D filter. Based on that response, various highpass, bandpass and bandstop filters can be developed.

The paper is organized as follows. Section 2 gives the impulse responses of a separable filter with an ideal rectangular passband and of a non-separable filter with an ideal spherical passband. Section 3 summarizes the results and a separate Appendix section outlines the derivation of the results in Section 2.

2. IDEAL LOWPASS FILTER

The starting point for designing a filter is the ideal lowpass filter spectral characteristic from which different highpass, bandpass and bandstop filter configurations can be derived. Similarly to the digital filters in 2-D signal and image processing [1, 2], the 3-D image filters can also be separable with rectangular support and non-separable. The non-separable 3-D filter considered in this paper has a circular support.

The performance difference between a separable and a non-separable filter lies in the spectral characteristics along different directions in 3-D space. On the one hand, the separable filter is simply designed; its impulse response is equal to the product of the marginal impulse responses along the three spatial axes which determines independent spectral characteristics along the three axes. Its passband is rectangular which means that this kind of filter would pass higher frequencies along the diagonal directions of the rectangle, compared to the frequencies along each frequency axis.

On the other hand, the non-separable filter offers spectral characteristics along the different directions which are no longer independent. In particular, the non-separable filter with spherical passband offers equal spectral characteristics along any direction in 3-D space. This may be very important especially in computed tomography and magnetic resonance imaging where the data details are equally important in all directions.

Those observations give grounds to develop filter characterizations for both separable and non-separable 3-D filters. The particular use of one of them is determined by such factors as complexity, speed, reliability in all directions and, of course, the particular intended application.

2.1. Rectangular passband

The rectangular passband defines a separable 3-D filter. The impulse response of such a filter is given by (details in Appendix A)

$$h_r(n_1, n_2, n_3) = \frac{\sin \omega_{c_1} n_1}{\pi n_1} \frac{\sin \omega_{c_2} n_2}{\pi n_2} \frac{\sin \omega_{c_3} n_3}{\pi n_3} \quad (1)$$

for $-\infty < n_1, n_2, n_3 < \infty$, where $\omega_{c_1}, \omega_{c_2}$ and ω_{c_3} are the cut-off spatial frequencies along the corresponding three frequency axes.

For $\omega_{c_1} = \omega_{c_2} = \omega_{c_3} = \omega_c$, the filter's passband becomes cubic.

Fig. 1 shows pseudocolor slice plots of the impulse response of the separable 3-D filter in (1). Fig. 1a shows the rectangular passband 3-D filter with $\omega_{c_1} = \pi/2$, $\omega_{c_2} = \pi/4$ and $\omega_{c_3} = \pi/8$. Fig. 1b shows the cubic passband 3-D filter with the cut-off spatial frequency $\omega_c = \pi/4$.

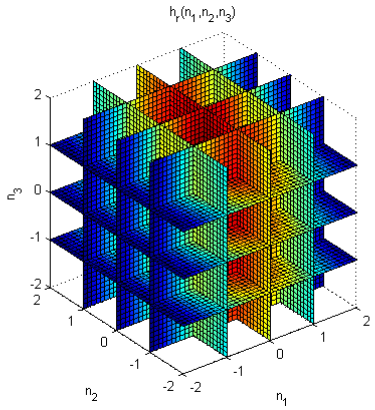

a) Rectangular passband with $\omega_{c_1} = \pi/2$, $\omega_{c_2} = \pi/4$ and $\omega_{c_3} = \pi/8$

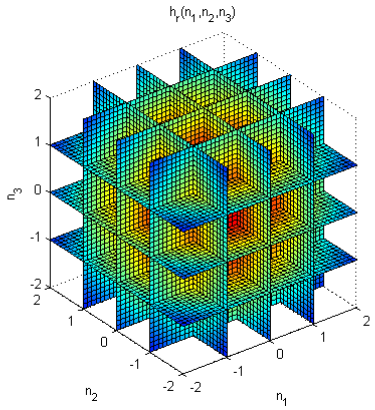

b) Cubic passband with $\omega_c = \pi/4$

Fig. 1. Impulse response of a separable 3-D filter with a rectangular passband

2.2. Spherical passband

The spherical passband defines a non-separable 3-D filter. The impulse response of such a filter is given by (details in Appendix B)

$$h_s(n_1,n_2,n_3) = \frac{\omega_c\, j_1\left(\omega_c\sqrt{n_1^2+n_2^2+n_3^2}\right)}{4\pi\left(n_1^2+n_2^2+n_3^2\right)} \qquad (2)$$

with $j_1(\bullet)$ being the first-order spherical Bessel function of the first kind and ω_c being the cut-off spatial frequency.

Fig. 2 shows s pseudocolor slice plot of the impulse response of the non-separable 3-D filter with spherical passband in (2) with cut-off spatial frequency $\omega_c = \pi/4$.

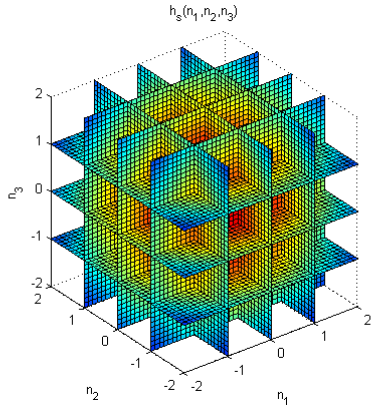

Fig. 2. Impulse response of a non-separable 3-D filter with a spherical passband

3. CONCLUSION

This paper develops derivation of the impulse responses for a separable and a non-separable 3-D filters. The separable filter naturally has a rectangular passband while the non-separable filter considered here is with spherical passband. Such filters are applicable in 3-D and 4-D computed tomography imaging, as well as in various volumetric subsurface sensing and imaging applications. Further work will report various performance measures of those filters applied to different real-world captured data sets.

4. APPENDIX

A. Ideal lowpass filter with a rectangular passband

The frequency response of such a filter is given by

$$H_r(\omega_1,\omega_2,\omega_3) = I_{\omega_{c_1}}(\omega_1) I_{\omega_{c_2}}(\omega_2) I_{\omega_{c_3}}(\omega_3) \qquad (3)$$

in the frequency cube $[-\pi,+\pi]^3$, where the indicator function $I_{\omega_{c_i}}$ is defined as

$$I_{\omega_{c_i}} \triangleq \begin{cases} 1, & |\omega| \le \omega_{c_i}, \\ 0, & \text{else}, \end{cases} \qquad (4)$$

for l = 1, 2, 3, and with ω_{c_i} being the filter's cut-off frequency with $\left|\omega_{c_i}\right| \le \pi$. The ideal impulse response of the filter is derived by taking the inverse 3-D Fourier transform of this separable function in the frequency domain:

$$\begin{aligned} h_r &= \frac{1}{(2\pi)^3}\int_{-\pi}^{\pi}\int_{-\pi}^{\pi} 1 e^{j(\omega_1 n_1+\omega_2 n_2+\omega_3 n_3)} d\omega_1 d\omega_2 d\omega_3 \\ &= \left[\frac{1}{2\pi}\int_{-\pi}^{\pi} I_{\omega_{c_1}}(\omega_1) e^{j\omega_1 n_1} d\omega_1\right] \\ &\times \left[\frac{1}{2\pi}\int_{-\pi}^{\pi} I_{\omega_{c_2}}(\omega_2) e^{j\omega_2 n_2} d\omega_2\right] \\ &\times \left[\frac{1}{2\pi}\int_{-\pi}^{\pi} I_{\omega_{c_3}}(\omega_3) e^{j\omega_3 n_3} d\omega_3\right] \\ &= \frac{\sin\omega_{c_1} n_1}{\pi n_1}\frac{\sin\omega_{c_2} n_2}{\pi n_2}\frac{\sin\omega_{c_3} n_3}{\pi n_3}, \end{aligned} \quad (5)$$

for $-\infty < n_1, n_2, n_3 < \infty$.

B. Ideal lowpass filter with a spherical passband

The frequency response of such a filter is given by

$$H_s(\omega_1,\omega_2,\omega_3) = \begin{cases} 1, & \sqrt{\omega_1+\omega_2+\omega_3} \le \omega_c, \\ 0, & \text{else}, \end{cases} \quad (6)$$

in the frequency cube $[-\pi,+\pi]^3$. The ideal impulse response of the filter is derived by taking the inverse 3-D Fourier transform of this function in the frequency domain:

$$\begin{aligned} h_s &= \frac{1}{(2\pi)^3}\iiint_{\sqrt{\omega_1+\omega_2+\omega_3}\le\omega_c} 1 e^{j(\omega_1 n_1+\omega_2 n_2+\omega_3 n_3)} d\omega_1 d\omega_2 d\omega_3 \\ &= \frac{1}{(2\pi)^3}\int_0^{\omega_c}\int_0^{\pi}\int_0^{2\pi} e^{jur\begin{pmatrix}\sin\psi\sin\varphi\cos\phi\cos\theta \\ +\sin\psi\sin\varphi\sin\phi\sin\theta \\ +\cos\psi\cos\varphi\end{pmatrix}} u^2\sin\varphi\, du\, d\theta\, d\varphi \\ &= \frac{1}{(2\pi)^3}\int_0^{\omega_c}\int_0^{\pi}\int_0^{2\pi} e^{jur\begin{pmatrix}\sin\psi\sin\varphi\cos(\theta-\phi) \\ +\cos\psi\cos\varphi\end{pmatrix}} u^2\sin\varphi\, du\, d\theta\, d\varphi \\ &= \frac{1}{(2\pi)^2}\int_0^{\omega_c} u^2\int_0^{\pi} e^{jur\cos\varphi}\sin\varphi\, d\varphi\, du \\ &= \frac{1}{4\pi}\int_0^{\omega_c} u^2 j_0(ur)\, du = \frac{\omega_c j_1\left(\omega_c\sqrt{n_1^2+n_2^2+n_3^2}\right)}{4\pi\sqrt{n_1^2+n_2^2+n_3^2}} \end{aligned} \quad (7)$$

where $j_0(\bullet)$ and $j_1(\bullet)$ are the zero-order and the first-order spherical Bessel functions of the first kind [3].

In order to carry out the integration, the following substitutions have been made. First, polar coordinates in frequency are used for $\omega_1 = u\sin\psi\cos\theta$, $\omega_2 = u\sin\psi\sin\theta$ and $\omega_3 = u\cos\psi$. Then, polar coordinates in space are used for $n_1 = r\sin\varphi\cos\phi$, $n_2 = r\sin\varphi\sin\phi$ and $n_3 = r\cos\varphi$.

References

[1] J. Woods, Multidimensional signal, image and video processing and coding, Elsevier Academic Press, 2006.

[2] D. Dudgeon, R. Mersereau, Multidimensional digital signal processing, Prentice Hall, 1990.

[3] M. Abramowitz, I. Stegun, Handbook of mathematical functions with formulas, graphs and mathematical tables, Dover, 1972.